Carotid vasa vasorum detected by super-resolution ultrasound microvascular imaging in Takayasu's arteritis: a potential biomarker of disease activity and early treatment outcome

P. Cong[1], C.-X. Li[1], C.-K. Zhao[1], T.-T. Fu[1,2], P. Sun[1,2], K.-L. Chen[1,2], Y.-L. Zhu[1,2], Y.-Q. Zhang[1,2], D. Lu[1,2], Y.-W. Luo[1,2], S.-J. You[1,2], L.-Y. Ma[3], L.-D. Jiang[3], H. Han[1], H.-X. Xu[1]

[1]Department of Ultrasound, Zhongshan Hospital, Fudan University, Shanghai;
[2]Shanghai Institute of Medical Imaging, Shanghai;
[3]Department of Rheumatology, Zhongshan Hospital, Fudan University, Shanghai, China.

Abstract

Objective

To verify the ability of super-resolution ultrasound (SRUS) microvascular imaging in assessing Takayasu's arteritis (TAK) activity and predicting prognosis.

Methods

Between November 2023 and July 2024, 70 patients with TAK were consecutively included; disease activity was assessed per the 1990 American College of Rheumatology classification criteria (26 active, 44 inactive). B-mode ultrasound (US), conventional contrast-enhanced ultrasound (CEUS), and SRUS microvascular imaging examinations were performed at the carotid site with maximal wall involvement using the Resona A20 system equipped with a SL10-3U linear transducer. We compared diagnostic performance of individual markers and combined models for disease activity and evaluated deterioration-free survival with Kaplan-Meier analysis.

Results

Carotid vasa vasorum was detected by SRUS microvascular imaging in 14 patients (11 active, 3 inactive), while it was not observed in the remaining 56 cases (41 inactive, 15 active). Presence of vasa vasorum correlated strongly with disease activity ($p<0.001$), demonstrating 42.3% sensitivity, 93.2% specificity, and 74.3% accuracy. The prediction model constructed based on clinical and US characteristics demonstrated high accuracy in assessing TAK activity (area under the curve=0.900). Among 41 patients completing follow-up (17 active, 24 inactive; mean 8.7±2.7 months), patients with inactive TAK maintained stable disease (only 1 relapsed to active phase). Among patients with active TAK, those with vasa vasorum demonstrated significantly poorer outcomes: only 2/7 (28.6%) achieved remission versus 9/10 (90%) without vasa vasorum ($p=0.036$).

Conclusion

SRUS detection of carotid vasa vasorum serves as a useful indicator for assessing the activity and severity of TAK.

Key words

Takayasu's arteritis, vasa vasorum, carotid artery diseases, diagnostic imaging, ultrasonography, sensitivity and specificity, predictive value of tests

*Peng Cong, MM**
*Cui-Xian Li, MD**
Chong-Ke Zhao, MD
Tian-Tian Fu, MM
Pei Sun, MM
Kai-Ling Chen, MD
Yu-Li Zhu, MD
Ya-Qin Zhang, MM
Dan Lu, MM
Yan-Wen Luo, MD
Su-Jun You, MM
Ling-Ying Ma, MD
Lin-Di Jiang, MD
Hong Han, MD
Hui-Xiong Xu, MD

**Contributed equally.*

Please address correspondence to:
Hong Han
Department of Ultrasound,
Zhongshan Hospital,
Fudan University,
no. 180 Fenglin Road, Xuhui District,
Shanghai 200032, China.
E-mail: han.hong@zs-hospital.sh.cn

and to:
Hui-Xiong Xu,
(same postal address)
E-mail: xuhuixiong@126.com.

Chong-Ke Zhao,
(same postal address)
E-mail: zhaochongke123@163.com.

Received on July 20, 2025; accepted in revised form on October 13, 2025.

Funding: this study has received funding by the National Natural Science Foundation of China (grant 82202174, 82430064, and 82572222), Horizontal Project of Zhongshan Hospital of Fudan University (H2024-077), Scientific Research and Development Fund of Zhongshan Hospital of Fudan University (grant 2022ZSQD07), and Medical Engineering fund of Fudan University (grant IDH2310157).

Competing interests: none declared.

Introduction

Takayasu's arteritis (TAK) is a rare chronic large-vessel vasculitis predominantly affecting young women (1). The disease primarily targets the aorta and its major branches, manifesting histologically as granulomatous inflammation of the vascular wall (2). Carotid involvement represents the most prevalent vascular manifestation in TAK, affecting 45–84% of patients (3). Characterised by an insidious disease onset, TAK frequently presents with non-specific constitutional symptoms such as fatigue, low-grade fever, and arthralgia during the early 'pre-pulseless' phase (4). This clinical ambiguity complicates diagnosis and often delays therapeutic intervention. Inadequately treated TAK is associated with higher disability and mortality compared to the general population (5).

Imaging modalities including ultrasound (US), computed tomography angiography (CTA), and magnetic resonance angiography (MRA) play a critical role in distinguishing active from inactive TAK and thereby guide clinical management and tailored treatment regimens (6-8). Specifically, US has been validated as a reliable modality for evaluating vascular involvement in large-vessel vasculitis and is also recognised as the most effective method for carotid assessment (9, 10). Among US techniques, contrast-enhanced ultrasound (CEUS) can demonstrate carotid wall neovascularisation and serve as a potential biomarker of disease activity in patients with TAK (11). Conventional CEUS, however, infers microcirculatory changes indirectly through the degree of enhancement produced by the intravascular contrast agent, rather than by directly visualising the carotid vasa vasorum (12). Furthermore, the interpretation of CEUS findings remains operator-dependent, introducing inherent subjectivity in evaluations.

Super-resolution ultrasound (SRUS) microvascular imaging achieves unprecedented visualisation of microvascular architecture by continuously tracking and localising microbubble (MB) centroids within the vascular lumen at sub-wavelength spatial resolution (13, 14). SRUS overcomes the diffraction limit inherent to conventional US and enables non-invasive assessment of tissue perfusion at microscopic scales, permitting quantitative analysis of haemodynamic parameters (15). Researchers have applied SRUS microvascular imaging preliminarily to cerebrovascular imaging (16), atherosclerotic plaque assessment (17), and renal disease evaluation (18). Prior reports indicate that SRUS can directly visualise carotid vasa vasorum in patients with active TAK, providing critical insights into TAK assessment (19, 20). Nevertheless, existing studies remain limited by small cohort sizes (<20 cases), insufficient exploration of correlations between SRUS microvascular imaging features and clinical parameters, and lack of longitudinal follow-up to assess prognostic implications of imaging findings.

The objective of this study was to perform SRUS microvascular imaging examinations in patients with TAK exhibiting carotid involvement and to verify the ability of this technique in assessing disease activity and predicting prognosis.

Materials and methods

Participants

We recruited consecutive patients with TAK from Zhongshan Hospital, Fudan University between November 2023 and July 2024.

Inclusion criteria were as follows:
(a) patients aged ≥18 years; (b) those with TAK diagnosis fulfilling the 1990 American College of Rheumatology (ACR) classification criteria (21); and (c) those with radiologically confirmed carotid involvement by CTA or MRA.

Exclusion criteria were as follows:
(a) patients with contraindications to US contrast agents; (b) those with suboptimal image quality or incomplete clinical data; and (c) those that declined study participation.

The Clinical Research Ethics Committee of Zhongshan Hospital, Fudan University approved the study protocol (approval no.: B2022-189). We obtained written informed consent obtained from all participants prior to enrolment. The study procedures were conducted in accordance with the tents of the Helsinki Declaration of 1983.

B-mode US images acquisition

We performed US examinations using the Resona A20 system (Mindray Bio-Medical Electronics Co., Ltd., Shenzhen, China) equipped with an SL10-3U linear transducer. A vascular US specialist (HH >10 years of clinical experience), conducted all examinations and remained blinded to participants' clinical histories throughout the study. Participants were positioned supine with adequate neck exposure and then bilateral carotid arteries were systematically scanned in both longitudinal and transverse planes. We identified the arterial segment with maximal wall thickness as the most prominent lesion and measured carotid wall thickness, internal diameter, and external diameter at that site.

CEUS images acquisition

We administered contrast agent via antecubital venous access using 1.5 mL SonoVue (Bracco, Milan, Italy), followed by a 5 mL saline flush to optimise microbubble (MB) circulation. CEUS acquisition focused on the most prominent lesion, maintaining strict centring within the imaging plane. Dynamic contrast enhancement was continuously recorded for 120 seconds after contrast agent injection.

SRUS microvascular imaging acquisition

After 15 min of the first CEUS, the contrast agent was essentially undetectable within the carotid artery. Subsequently, a second bolus of 1.5 mL SonoVue was administered via the antecubital vein. The SRUS microvascular imaging mode was activated, focusing on the most prominent lesion. When B-mode imaging visually confirmed MBs in the carotid lumen, we instructed participants to hold their breath to minimise motion artifacts. We stabilised the probe and collected dynamic images for 6 s.

Interpretation of CEUS and SRUS microvascular imaging

Three radiologists independently interpreted CEUS and SRUS microvascular imaging: a senior radiologist (HH with >10 years of experience), a mid-level radiologist (TTF with 5 years of experience); and a junior radiologist (PC with 2 years of experience). The senior radiologist trained the other two radiologists in the interpretation of carotid CEUS and SRUS microvascular imaging before study initiation. The three radiologists jointly analysed images from 20 patients with TAK, who were not included in the present cohort, to standardise interpretation. We designated the senior radiologist's interpretation as the definitive assessment.

We graded CEUS semi-quantitatively as follows: Grade 0: no vascularisation (absence of MB within the lesion); Grade 1: limited vascularisation (limited visualisation of moving MB in the lesion); Grade 2: moderate vascularisation (moderate visualisation of moving MB in the lesion); Grade 3: severe vascularisation (extensive wall vascularisation with MBs clearly seen). Carotid wall enhancement on CEUS correlates with histologically confirmed neovascularisation; greater enhancement corresponds to higher micro vessel density (22). We adopted a visual CEUS grade of carotid wall enhancement ≥2 as indicative of active TAK, a threshold shown to have optimal diagnostic performance in prior studies (11, 23).

We performed SRUS microvascular imaging analysis using qualitative and quantitative approaches. For qualitative assessment, we classified vasa vasorum within carotid walls as present or absent. For quantitative assessment, we measured vasa vasorum density, flow-weighted vessel density, and additional parameters in the most prominent lesions using SR-CEUS V3 software (Mindray Bio-Medical Electronics Co., Ltd., Shenzhen, China) on a dedicated workstation.

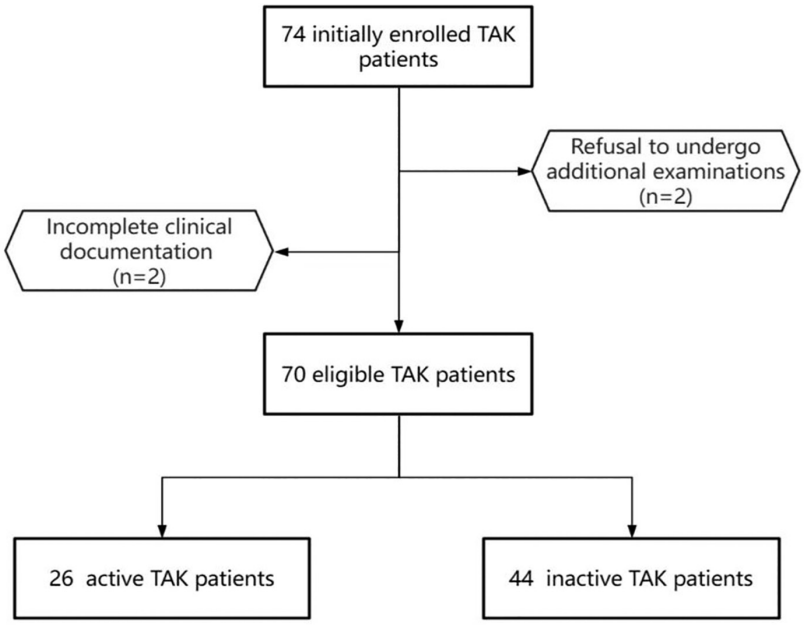

Fig. 1. Flowchart for patient recruitment in this study.
TAK: Takayasu's arteritis.

Clinical evaluation and treatment

All enrolled patients underwent comprehensive clinical, laboratory, and imaging evaluations within one week following initial assessment. Two experienced rheumatologists recorded the patients' clinical data and evaluated disease activity according to the National Institute of Health (NIH) score (24), which includes four criteria: (a) systemic features such as fever and musculoskeletal symptoms (no other cause identified); (b) elevated erythrocyte sedimentation rate (ESR); (c) features of vascular ischaemia or inflammation, such as claudication, diminished or absent pulse, bruit, vascular pain (carotidynia), or asymmetric blood pressure in either upper or lower limbs (or both); and (d) typical angiographic features. New onset or worsening of at least two of these criteria indicates "active disease". Subsequently, the two

Table I. Demographic and clinical characteristics of patients with Takayasu's arteritis.

Characteristics	Active TAK group (n=26)	Inactive TAK group (n=44)	*p*
Sex			0.880
Male (n)	3	7	
Female (n)	23	37	
Age (years)	32.5 (15.3)	35 (17.5)	0.114
Laboratory findings			
Hb (g/L)	118.00 (22.75)	117.00 (11.50)	0.601
PLT ($\times 10^9$/L)	278.00 (171.75)	229.00 (100.00)	0.111
WBC ($\times 10^9$/L)	7.84 ± 2.43	7.86 ± 2.39	0.945
ESR (mm/hour)	16.00 (21.50)	7.00 (7.00)	0.003*
CRP (mg/L)	2.45 (20.35)	1.00 (6.40)	0.021*
IL-6 (pg/mL)	5.10 (5.58)	3.00 (2.60)	0.007*
TNF (pg/mL)	11.55 (7.43)	10.35 (6.45)	0.208
NIH score details			
Systemic symptoms (n)	16	8	<0.001*
Ischaemia or vascular inflammation (n)	19	6	<0.001*
Acute-phase reactant elevation (n)	9	0	<0.001*
Angiographic features (n)	19	8	<0.001*

TAK: Takayasu's arteritis; Hb: haemoglobin; PLT: platelet; WBC: white blood cell; ESR: erythrocyte sedimentation rate; CRP: C-reactive protein; IL-6: interleukin-6; TNF: tumour necrosis factor.
Values are expressed as numbers (percentages) or as means (standard deviations).
*p-values indicate statistical significance ($p<0.05$).

Table II. US characteristics of patients with Takayasu's arteritis.

Characteristics	Active TAK group (n=26)	Inactive TAK group (n=44)	*p*
B-mode US			
Artery wall thickness (mm)	2.10 (0.85)	1.50 (0.60)	<0.001*
External diameter (mm)	7.55 (2.18)	6.70 (2.15)	0.042*
Internal diameter (mm)	3.50 ± 2.16	3.88 ± 2.37	0.925
Conventional CEUS			<0.001*
Grade 0	0	13	
Grade 1	6	23	
Grade 2	11	8	
Grade 3	9	0	
SRUS microvascular imaging			<0.001*
Presence of vasa vasorum	11	3	
Absence of vasa vasorum	15	41	

SRUS: super-resolution ultrasound.
Values are expressed as numbers (percentages) or as means (standard deviations).
* p-values indicate statistical significance ($p<0.05$).

physicians formulated corresponding treatment plans for the patients.

After treatment, the same rheumatologists evaluated prognosis. We determined complete remission if the following four criteria were satisfied: (a) absence of new or worsened systemic symptoms; (b) absence of new or worsened vascular symptoms or signs; (c) ESR within normal limits (≤40 mm/h); (d) glucocorticoid dose ≤15 mg/day. Partial remission was defined as fulfilment of criterion (b) along with any two of the criteria (a), (c), or (d). We defined relapse as reactivation of disease activity meeting NIH criteria (≥2 points) in patients who previously achieved complete or partial remission (25). Disease progression was defined as persistent active disease throughout treatment without achieving complete or partial remission. Both relapse and progression were classified as clinical deterioration. The two rheumatologists remained blinded to US findings during all clinical assessments.

Statistical analysis

Statistical analyses were performed using SPSS (v. 25.0, IBM SPSS Statistics) and R (v. 4.5.0, R Foundation for Statistical Computing, Vienna, Austria) software. Normally distributed continuous variables were expressed as mean ± standard deviation and compared using independent samples t-tests. Non-normally distributed continuous variables were reported as median (interquartile range, IQR) and analysed via Mann-Whitney U-tests. Categorical variables were presented as frequencies or percentages (%) and compared using chi-square or Fisher's exact tests as appropriate. Multivariate logistic regression analysis was conducted on variables demonstrating p-value <0.1 in univariate analysis to develop a combined prediction model. R packages '*rms*', '*pROC*', and '*ggplot2*' were used to build a nomogram for model visualisation. We generated receiver operating characteristic (ROC) curves, and calculated area under the curve (AUC) values to assess model performance. Model performance differences were evaluated using DeLong's test. The accuracy of the prediction model was evaluated using the Hosmer-Lemeshow test and a calibration plot. Interobserver agreement among the three radiologists was quantified through Kappa analysis: $\kappa<0.20$ suggests poor agreement, $0.20\leq \kappa \leq 0.40$ suggests fair agreement, $0.40< \kappa \leq 0.60$ suggests moderate agreement, $0.60 <\kappa\leq 0.80$ suggests substantial agreement, and $\kappa >0.80$ suggests almost perfect agreement. Deterioration-free survival was evaluated using Kaplan-Meier methodology with log-rank testing for between-group comparisons. A p-value of <0.05 was considered statistically significant.

Results

Demographic and clinical characteristics of patients with TAK

Among 74 initially enrolled patients, four were excluded for the following reasons: refusal to undergo additional examinations (n=2), and incomplete clinical documentation (n=2). Consequently, 70 patients with TAK (age range: 19–76 years; 85.7% female) were included in the final analysis (Fig. 1). Baseline characteristics of the cohort are summarised in Table I. Comparative analysis revealed no significant differences in sex distribution or age between patients with active TAK (n=26) and inactive TAK (n=44). However, inflammatory biomarkers includ-

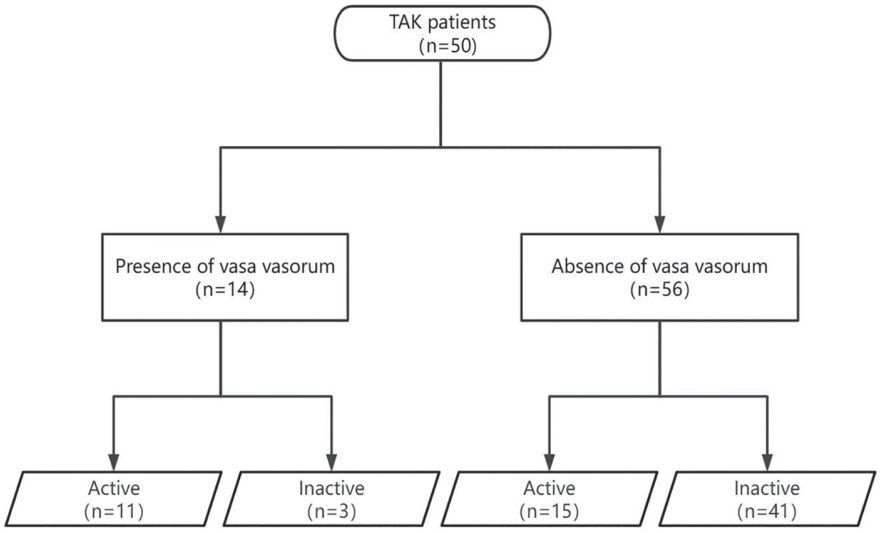

Fig. 2. Stratification of patients with Takayasu's arteritis based on the detection of carotid vasa vasorum using super-resolution ultrasound microvascular imaging.
TAK: Takayasu's arteritis.

ing ESR (p=0.003), C-reactive protein (CRP, p=0.021), and interleukin-6 (IL-6, p=0.007) demonstrated significant associations with disease activity.

Comparison of US characteristics between patients with active TAK and those with inactive TAK

Table II summarises US characteristics of the cohort. On B-mode US, patients in the active group exhibited significantly greater carotid wall thickness compared to the inactive group (median [IQR]: 2.10 [0.85] mm *vs*. 1.50 [0.60] mm, respectively; p<0.001) and external diameter (7.55 [2.18] mm *vs*. 6.70 [2.15] mm, respectively; p=0.042). CEUS analysis revealed higher MB enhancement grades in active TAK patients (p<0.001). SRUS microvascular imaging detected carotid vasa vasorum at a significantly higher frequency in patients with active TAK compared to those with inactive TAK (p<0.001).

SRUS microvascular imaging detection of vasa vasorum correlates with TAK activity

In the present cohort, SRUS microvascular imaging detected carotid vasa vasorum in 14 patients, 11 of whom (78.6%) were in active phase; of the remaining 56 patients without detectable carotid vasa vasorum, 41 (73.2%) were in the inactive phase.

This imaging biomarker demonstrated 42.3% sensitivity (95% CI: 24.3–61.7%) and 93.2% specificity (95% CI: 81.8–99.1%) for identifying active TAK, with overall accuracy of 74.3% (Table II and Fig. 2, 3).

Prediction model for TAK activity

We constructed a logistic regression model using clinical and US characteristics associated with TAK activity (Fig. 4a). AUC values for individual predictors were as follows: ESR=0.710; IL-6=0.694; artery wall thickness =0.752; conventional CEUS=0.859; SRUS microvascular imaging =0.677; and the combined prediction model =0.900 (Fig. 4b). The performance of the combined prediction model was signifi-

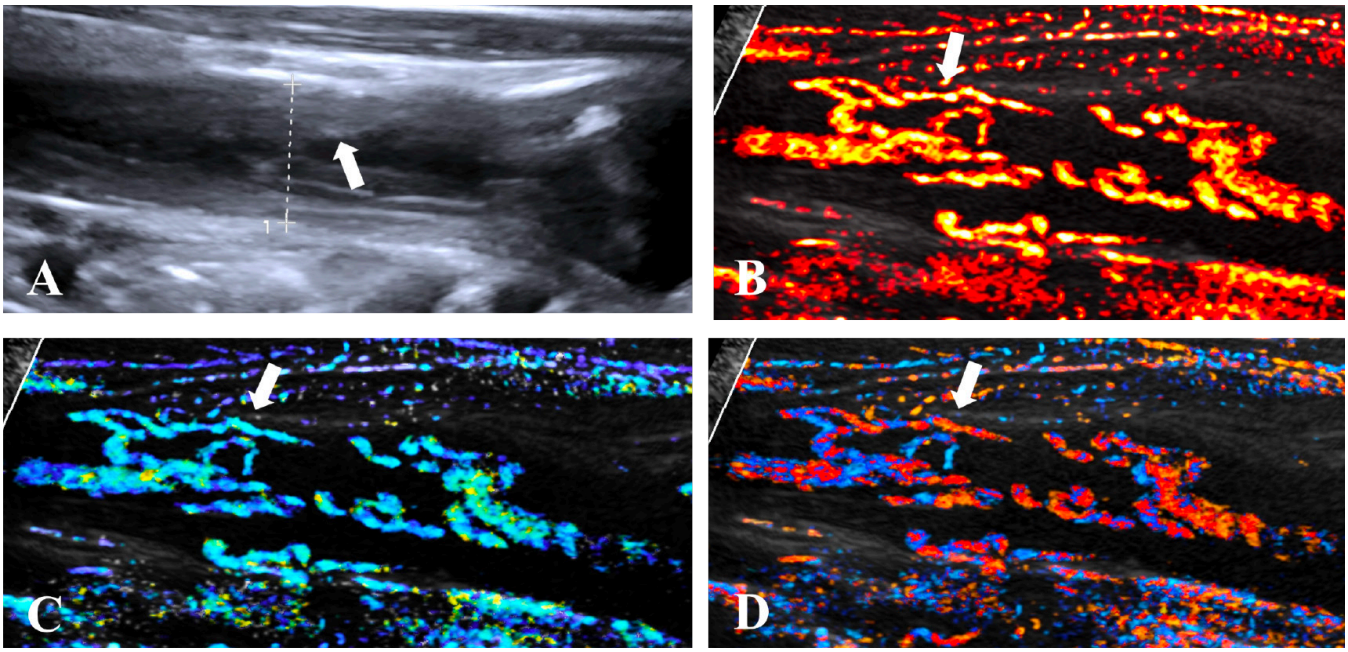

Fig. 3. Representative super-resolution ultrasound (SRUS) microvascular imaging of carotid vasa vasorum in Takayasu's arteritis.
A: B-mode US demonstrates obvious irregular thickening of carotid artery wall (white arrow). **B-D**: SRUS microvascular imaging parametric maps reveal vasa vasorum within the thickened arterial wall (white arrows). **B**: Vessel density map. **C**: Flow velocity map. **D**: Flow direction map.

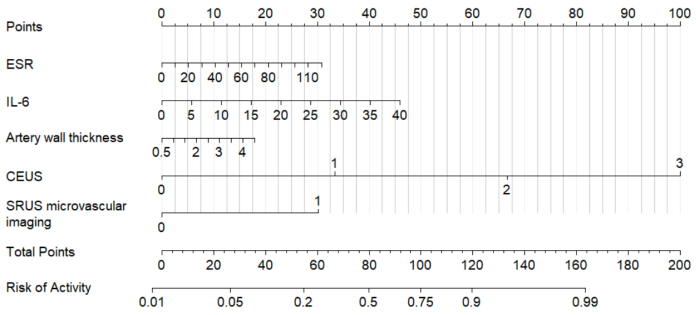

A

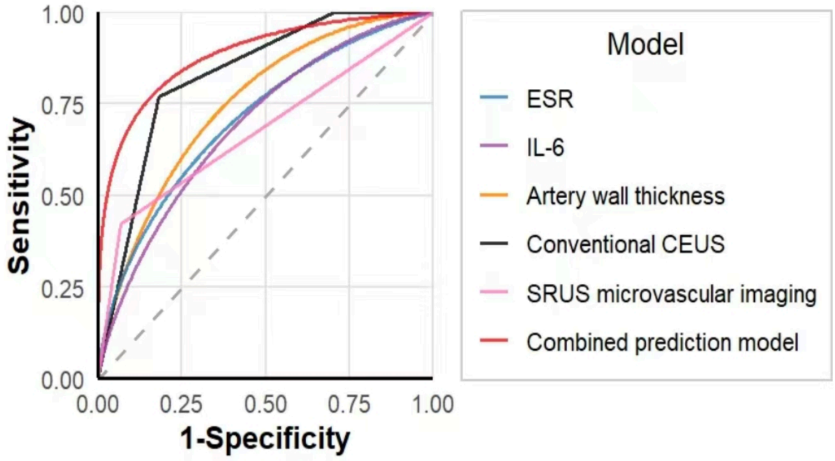

B

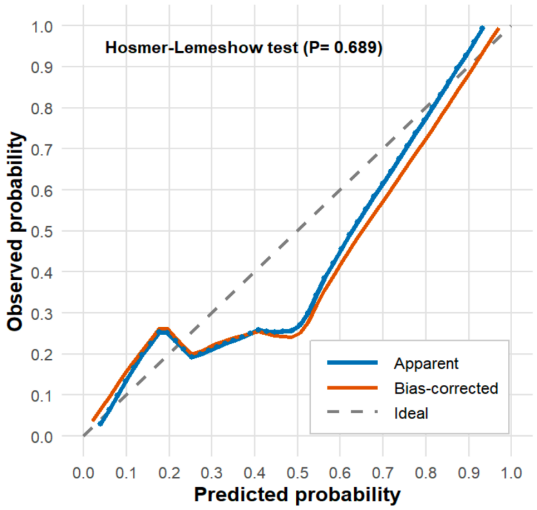

C

Fig. 4. A: Nomogram for predicting the risk of Takayasu's arteritis activity. **B**: Performance evaluation of individual factors and the combined prediction model in assessing Takayasu's arteritis activity. **C**: Calibration plot for the combined prediction model.
ESR: erythrocyte sedimentation rate; IL-6: interleukin-6; SRUS: super-resolution ultrasound.

cantly superior to all individual factors (p<0.05 for all comparisons). The calibration plot was developed for the combined prediction model and subjected to the Hosmer-Lemeshow test (p=0.689), indicating good model fit (Fig. 4c).

Quantitative analysis based on SRUS microvascular imaging

We performed quantitative analysis using SRUS microvascular imaging data of 14 patients with TAK, focusing specifically on the carotid vasa vasorum. Results demonstrated significantly higher median vessel density (p=0.036) and flow-weighted vessel density (p=0.036) in patients with active TAK compared to those with inactive disease (Table III). No statistically significant differences were observed for the other parameters (p>0.05).

SRUS microvascular imaging detection of vasa vasorum correlates with the severity of active TAK

We sub-stratified 26 patients with active TAK based on SRUS microvascular imaging detection of carotid vasa vasorum. As detailed in Table IV, patients with carotid vasa vasorum exhibited younger age (24 [11] *vs*. 34 [20] years, respectively; p=0.041) and higher NIH scores (p=0.011) compared to those without detectable vasa vasorum. These findings suggest that active TAK with carotid vasa vasorum represent a distinct clinical phenotype characterised by earlier disease onset and more severe vasculitic manifestations.

SRUS microvascular imaging detection of vasa vasorum correlates with the prognosis of active TAK

All enrolled patients received standardised therapy, with 41 patients (17 with active and 24 with inactive disease) completing follow-up between 3.4–13.6 months (mean 8.7±2.7 months) post-enrolment.

The prognosis of 24 patients with inactive TAK was relatively stable; only one (4.2%) relapsed to the active phase. We divided 17 patients with active disease into two groups based on the detection of carotid vasa vasorum in SRUS microvascular imaging (Table V). Patients with vasa vasorum had elevated levels of IL-6 after treatment (p=0.043). Significant outcome disparities were observed: only 2/7 (28.6%) patients in the active group with vasa vasorum achieved partial remission, compared to 9/10 (90%) patients in the active group without vasa vasorum attaining complete or partial remission (p=0.036). However, Kaplan-Meier analysis of deterioration-free survival showed no significant intergroup divergence (log-rank p=0.695) (Fig. 5). Figures 6 and 7

Table III. Comparison of quantitative parameters of carotid vasa vasorum between patients with active Takayasu's arteritis and those with inactive disease.

Parameters	Active TAK group (n=11)	Inactive TAK group (n=3)	*p*
Vessel density			
Maximum density	3.27 (2.29)	2.36	0.312
Minimum density	0.01 (0.00)	0.01	1.000
Median density	0.60 (0.12)	0.37	0.036*
Density standard deviation	0.98 (0.74)	0.79	0.456
Flow-weighted vessel density	1.04 (0.89)	0.51	0.036*
Fractal dimension	1.43 (0.11)	1.40	0.697
Velocity (mm/s)			
Maximum velocity (mm/s)	43.81 (32.33)	50.82	0.697
Minimum velocity (mm/s)	2.25 (22.17)	1.84	0.484
Mean velocity (mm/s)	23.57 (21.95)	19.38	0.484
Velocity variance	112.43 (142.88)	245.40	0.102
Velocity entropy	0.75 (0.41)	0.64	0.210
Direction variance	2699.35 (3387.89)	5759.15	0.243
Direction entropy	0.61 (0.40)	0.53	0.138
Perfusion index	12.95 (17.29)	7.53	0.243

*p-values indicate statistical significance ($p<0.05$).
Values are expressed as numbers (percentages).

Table IV. Clinical and US characteristics of patients with active Takayasu's arteritis, with and without carotid vasa vasorum detected by SRUS microvascular imaging.

Characteristics	Group with vasa vasorum detected (n=11)	Group without vasa vasorum (n=15)	*p*
Sex			0.774
Male (n)	2	1	
Female (n)	9	14	
Age (years)	24.0 (11.0)	34.0 (20.0)	0.041*
Laboratory findings			
Hb (g/L)	115.36 ± 14.79	115.6 ± 17.46	0.500
PLT ($\times10^9$/L)	319.27 ± 85.34	278.67 ± 135.41	0.229
WBC ($\times10^9$/L)	7.80 ± 2.51	7.86 ± 2.46	0.909
ESR (mm/hour)	24.00 (32.00)	13.00 (12.00)	0.217
CRP (mg/L)	18.70 (28.50)	2.10 (13.40)	0.198
IL-6 (pg/mL)	5.00 (9.10)	5.20 (3.70)	0.574
TNF (pg/mL)	13.30 (46.80)	11.00 (3.50)	0.305
B-mode US			
Artery wall thickness (mm)	2.47 ± 0.63	1.87 ± 0.53	0.937
External diameter (mm)	7.99 ± 2.04	7.25 ± 1.82	0.619
Internal diameter (mm)	3.32 ± 1.96	3.64 ± 2.35	0.357
NIH score			0.011*
2	5	14	
3	3	0	
4	3	1	

Hb: haemoglobin; PLT: platelet; WBC: white blood cell; ESR: erythrocyte sedimentation rate; CRP: C-reactive protein; IL-6: interleukin-6; TNF: tumour necrosis factor; SRUS: super-resolution ultrasound.
Values are expressed as numbers (percentages) or as means (standard deviations).
* p-values indicate statistical significance ($p<0.05$).

present pre- and post-treatment US images for two representative cases.

Consistency analysis of carotid vasa vasorum images interpreted by different observers

As summarised in Table VI, interobserver agreement for SRUS microvascular imaging interpretations demonstrated near-perfect consistency across experience levels (κ=0.954–1.000), whereas CEUS evaluations exhibited only moderate agreement (κ=0.454–0.651).

Clinical factors associated with SRUS microvascular imaging detection of carotid vasa vasorum

We stratified the 70 patients with TAK into two groups based on SRUS microvascular imaging detection of carotid vasa vasorum (Table VII). Patients with detectable microvasculature exhibited younger age (25.0 [12.8] *vs*. 35.0 [17.5] years, respectively; $p=0.010$), elevated inflammatory biomarkers (CRP: 4.35 [27.83*]* *vs*. 1.30 [7.98] mg/L, respectively, $p=0.028$; IL-6: 4.70 [6.70] *vs*. 3.20 [3.75] pg/mL, respectively; $p=0.032$), increased carotid wall thickness (2.30 [0.70] *vs*. 1.50 [0.58] mm, respectively; $p<0.001$), and higher NIH scores ($p<0.001$).

Binary multivariable logistic regression identified independent predictors of vasa vasorum detection via SRUS microvascular imaging: younger age (OR=10.200, 95% CI: 2.532–41.085), elevated IL-6 levels (OR=11.267, 95% CI: 1.379–92.066), increased carotid wall thickness (OR=53.182, 95% CI: 6.269–451.165), and higher NIH score (OR=10.022, 95% CI: 2.454–40.925) (Fig. 8).

Discussion

In this prospective study focusing on patients with TAK exhibiting carotid involvement, we demonstrated that carotid vasa vasorum detected by SRUS microvascular imaging had a significant correlation with clinical disease activity. Although this imaging biomarker demonstrated limited sensitivity (42.3%), its high specificity (93.2%) and overall accuracy (74.3%) underscore its diagnostic utility. The multifactorial prediction model demonstrated high accuracy in assessing TAK activity (AUC=0.900). Quantitative analysis based on SRUS microvascular imaging revealed significantly higher median vessel density ($p=0.036$) and flow-weighted vessel density ($p=0.036$) in active versus inactive TAK lesions. Subgroup analysis of patients with active TAK and detectable vasa vasorum identified a distinct phenotype characterised by younger age ($p=0.041$) and higher NIH scores ($p=0.011$). Next, we conducted a follow-up and found that patients with active TAK with detectable vasa vasorum on SRUS microvascular imaging exhibited poorer therapeutic outcomes, with only 28.6% achieving remission *versus* 90% in those without detectable vasa vasorum ($p=0.036$). In addition, SRUS microvascular imaging demon-

Table V. Comparison of characteristics between patients with active TAK at follow-up, with and without carotid vasa vasorum detected by SRUS microvascular imaging.

Characteristics	Group with vasa vasorum detected (n=7)	Group without vasa vasorum (n=10)	*p*
Sex			<0.732
Male (n)	2	1	
Female (n)	5	9	
Age (years)	30.6 ± 12.10	41.0 ± 16.9	0.434
Time interval of follow-up (months)	10.0 ± 2.8	7.8 ± 2.0	0.150
Changes in laboratory findings			
Hb (g/L)	1.43 ± 15.75	6.30 ± 14.35	0.740
PLT (×10^9/L)	-54.00 ± 63.74	-40.40 ± 91.79	0.610
WBC (×10^9/L)	0.19 ± 1.65	1.22 ± 2.57	0.192
ESR (mm/hour)	-12.71 ± 33.46	-6.20 ± 13.51	0.196
CRP (mg/L)	0.10 (8.50)	0.00 (10.18)	0.364
IL-6 (pg/mL)	2.00 (13.60)	-0.55 (3.88)	0.043*
TNF (pg/mL)	2.00 (49.70)	3.65 (25.08)	0.536
Changes in B-mode US			
Artery wall thickness (mm)	-0.20 (0.60)	0.00 (0.23)	0.070
External diameter (mm)	-1.00 (1.40)	0.00 (1.40)	0.088
Internal diameter (mm)	0.10 (0.10)	0.05 (0.55)	0.887
Changes in NIH score			0.016*
0	4	1	
-1	0	5	
-2	2	4	
-4	1	0	
Follow-up outcome			0.036*
Deterioration	5	1	
CR or PR	2	9	

TAK: Takayasu's arteritis; Hb: haemoglobin; PLT: platelet; WBC: white blood cell; ESR: erythrocyte sedimentation rate; CRP: C-reactive protein; IL-6: interleukin-6; TNF: tumour necrosis factor; CR: complete remission; PR: partial remission; SRUS: super-resolution ultrasound.
Values are expressed as numbers (percentages) or as means (standard deviations).
*p-values indicate statistical significance (p<0.05).

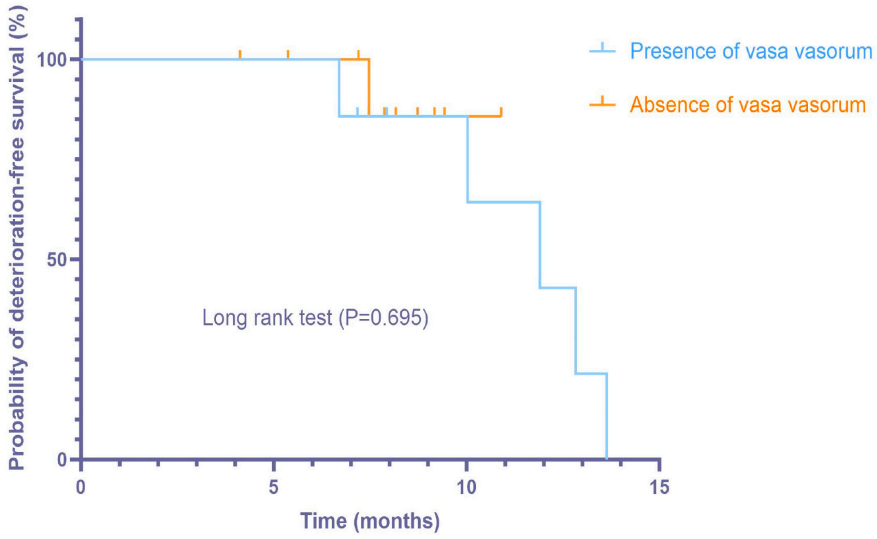

Fig. 5. Deterioration-free survival analysis in patients with active Takayasu's arteritis, with and without carotid vasa vasorum.

strated superior interobserver agreement (κ: 0.954–1.000) compared to CEUS (κ: 0.454–0.651), highlighting its reduced operator dependency. The following clinical factors were associated with SRUS microvascular imaging detection of carotid vasa vasorum: age (OR=10.200), IL-6 (OR=11.267), carotid wall thickness (OR=53.182), and NIH score (OR=10.022).

Neovascularisation of the carotid walls represents a characteristic histopathological feature of active TAK inflammation (26). CEUS can visualise microvascular signals within vascular walls, and Giordana *et al*. first reported its application in TAK in 2011 (27). Previous studies suggest that CEUS can assess carotid wall vascularisation by visualising MB traversing vascular walls (28, 29). However, emerging evidence from carotid plaque research indicates alternative mechanisms underlying CEUS enhancement, such as direct MB extravasation or macrophage-mediated transport, implying that CEUS enhancement may insufficiently reflect true neovascularisation (17). Furthermore, CEUS spatial resolution remains limited by ultrasound wavelength (approximately 200 μm), which precludes direct visualisation of microvascular features (15, 20). Therefore, non-invasive and precise detection of neovascularisation within the carotid wall remains a major challenge. SRUS microvascular imaging, adapted from optical super-resolution concepts, overcomes acoustic diffraction limits by localising MB trajectories at subwavelength resolution and thereby resolves microvascular architecture directly. SRUS generates quantitative vascular metrics that support objective disease assessment and can assist clinical decision-making (30). Goudot *et al*. proposed the feasibility of using SRUS microvascular imaging to evaluate TAK activity, reporting direct visualisation of carotid vasa vasorum and higher MB counts, MB-paths-per-second, and perfusion scores in active versus inactive TAK (19, 20).

In contrast to previous reports, our study revealed the following important findings. This study represented the first large-scale application of SRUS microvascular imaging in a TAK cohort, establishing a diagnostic profile characterised by moderate sensitivity and high specificity. The relatively low sensitivity of this technique could likely be attributed to the following two reasons: first, patients in whom SRUS detected carotid vasa vasorum were generally younger, had higher IL-6 levels, greater carotid wall thickness, and higher NIH scores, all of which were indicators reflecting the sever-

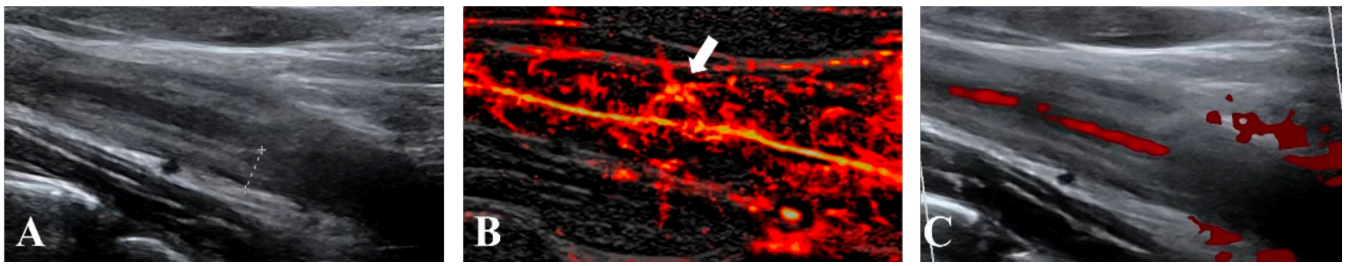

Fig. 6. Representative imaging of patients with active Takayasu's arteritis, with carotid vasa vasorum detected on super-resolution ultrasound (SRUS) microvascular imaging. **A**: Initial B-mode US (December 2023) demonstrates carotid wall thickening (4.00 mm). **B**: Concurrent SRUS microvascular imaging reveals vasa vasorum within the thickened artery wall (white arrow), correlating with active disease (NIH score: 3). **C**: Follow-up B-mode US imaging (Jun 2024) after 6.2 months of therapy shows persistent wall thickening (4.20 mm) with unabated inflammatory activity (NIH score: 3). NIH: National Institute of Health.

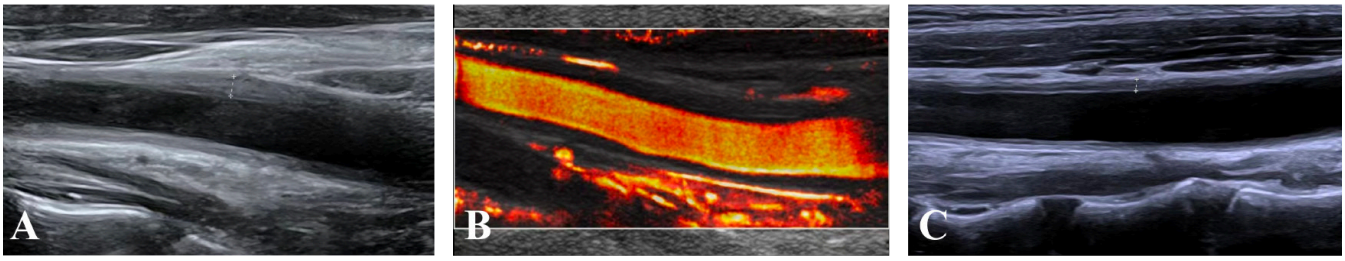

Fig. 7. Representative imaging of patients with active Takayasu's arteritis, without carotid vasa vasorum on super-resolution ultrasound (SRUS) microvascular imaging. **A**: Initial B-mode US (February 2024) demonstrates carotid wall thickening (1.90 mm). **B**: Concurrent SRUS microvascular imaging confirms absence of vasa vasorum within the thickened artery wall, and the NIH score of the patient is 2. **C**: Follow-up B-mode US imaging (Jul 2024) after 4.7 months of therapy shows artery wall thickness reduction (1.30 mm) and complete remission (NIH score: 0). NIH: National Institute of Health.

Table VI. Comparison of the consistency between carotid vasa vasorum images interpreted by radiologists with different levels of experience in patients with Takayasu arteritis.

	Senior radiologist	Mid-level radiologist	Junior radiologist	κ	*p*
SRUS microvascular imaging				1.000[a]	1.000[a]
Presence of vasa vasorum	14	14	13	0.954[b]	1.000[b]
Absence of vasa vasorum	56	56	57	0.954[c]	1.000[c]
Enhancement grade of carotid artery wall in CEUS				0.651[a]	0.388[a]
≥2	28	32	37	0.454[b]	1.000[b]
<2	42	38	33	0.509[c]	0.332[c]

SRUS: super-resolution ultrasound.
[a]senior radiologist *vs*. mid-level radiologist; [b] mid-level radiologist *vs*. junior radiologist, [c] senior radiologist *vs*. junior radiologist.

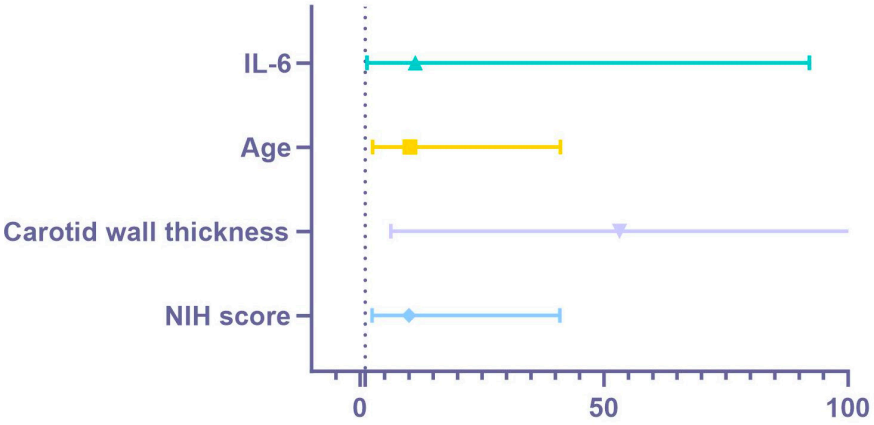

Fig. 8. Forest plot of four associated factors for detection of vasa vasorum within carotid walls by super-resolution ultrasound microvascular imaging in patients with Takayasu's arteritis.
IL-6: interleukin-6; NIH: National Institute of Health.

ity of the disease. Among 15 patients with active TAK in whom carotid vasa vasorum was not detected, nine had carotid artery wall thickness <2 mm and 14 had an NIH score of 2, suggesting that milder intramural involvement and minimal clinical activity reduce SRUS detectability. Second, SRUS microvascular imaging possesses inherent limitations, including susceptibility to motion artifacts from carotid pulsation and restriction to two-dimensional imaging planes, may impede detection of small or spatially complex vasa vasorum networks. These factors may account for the failure to detect carotid vasa vasorum in a subset of patients with active TAK.

Compared to conventional CEUS, SRUS microvascular imaging demonstrates excellent inter-observer agreement. Meanwhile, its operational workflow is highly comparable to that of conventional CEUS, allowing radiologists of varying experience levels to master the technique rapidly. These attributes favour clinical implementation.

Next, we investigated the prognostic significance of vasa vasorum detected on SRUS microvascular imaging: patients with active TAK exhibiting carotid vasa vasorum demonstrated 3.2-

Table VII. Clinical factors affecting the detection of carotid vasa vasorum by SRUS microvascular imaging.

Characteristics	Group with vasa vasorum detected (n=14)	Group without vasa vasorum (n=56)	*p*
Sex			1.000
Male (n)	2	8	
Female (n)	12	48	
Age (years)	25.0 (12.8)	35.0 (17.5)	0.010*
Laboratory findings			
Hb (g/L)	118.00 (17.50)	117.00 (12.75)	0.735
PLT ($\times 10^9$/L)	281.00 (157.75)	229.00 (92.75)	0.142
WBC ($\times 10^9$/L)	7.93 ± 2.55	7.83 ± 2.37	0.891
ESR (mm/hour)	17.00 (24.75)	8.00 (10.00)	0.076
CRP (mg/L)	4.35 (27.83)	1.30 (7.98)	0.028*
IL-6 (pg/mL)	4.70 (6.70)	3.20 (3.75)	0.032*
TNF (pg/mL)	11.20 (21.93)	10.65 (5.73)	0.872
B-mode US			
Artery wall thickness (mm)	2.30 (0.70)	1.50 (0.58)	<0.001*
External diameter (mm)	7.45 (3.40)	6.80 (2.18)	0.108
Internal diameter (mm)	3.58 ± 2.33	3.78 ± 2.29	0.973
NIH score			<0.001*
0	2	20	
1	1	21	
2	5	14	
3	3	0	
4	3	1	

Hb: haemoglobin; PLT: platelet; WBC: white blood cell; ESR: erythrocyte sedimentation rate; CRP: C-reactive protein; IL-6: interleukin-6; TNF: tumour necrosis factor; SRUS: super-resolution ultrasound. Values are expressed as numbers (percentages) or as means (standard deviations).
* *p*-values indicate statistical significance ($p<0.05$).

fold lower remission rates, providing a reference for predicting subsequent treatment outcomes and necessitating intensified surveillance in this high-risk subgroup.

In this study, CEUS semi-quantitative grading ≥2 demonstrated sensitivity and specificity of 76.9% and 81.8%, respectively, for identifying active TAK, roughly aligning with prior studies (23, 26, 29, 31). Compared to SRUS microvascular imaging, CEUS exhibited superior sensitivity but inferior specificity. Based on these findings, we recommend using a sequential diagnostic strategy: patients with CEUS grade ≥2 should undergo supplemental SRUS microvascular imaging examination to stratify disease severity, predict prognosis, and intensify follow-up intervals for those with detected carotid vasa vasorum.

Our study has several limitations that warrant consideration. First, the cohort size, while representing the largest SRUS microvascular imaging-TAK series to date, remains constrained by the rarity of TAK.

Second, the relatively short follow-up period may account for the lack of significant difference in the deterioration-free survival. We plan to conduct a follow-up study over 2 years to monitor changes in the patients' conditions in the future.

Lastly, this study is based on clinical data from real-world patients, without standardised therapeutic regimens; heterogeneity in medical management could introduce confounding. In the future, we will attempt to apply SRUS to a larger sample population and establish a more rigorous management process to minimise confounders, further clarifying the application value of SRUS microvascular imaging in the evaluation of TAK.

Conclusion

The detection of vasa vasorum within carotid artery walls via SRUS microvascular imaging serves as a useful indicator for assessing the activity and severity of TAK. This innovative modality not only enables high-resolution visualisation of microvascular architecture but also permits quantification of intraluminal haemodynamic, thereby providing critical insights for predicting disease prognosis and guiding personalised surveillance protocols. Further research should validate SRUS-based disease scoring system, optimise algorithms to reduce interference from carotid pulsations, leverage 3D imaging to improve the visualisation of carotid vasa vasorum, and integrate artificial intelligence technology for automated image analysis, feature extraction, and intelligent correction of motion artifacts to strengthen imaging support for advanced TAK investigation.

Acknowledgements

The authors thank all staff involved in this study and the patients and their families for their participation and co-operation.

References

1. UYSAL S, KALYONCU UCAR A, OZDEDE A *et al*.: Carotid artery ultrasonography and shear wave elastography in Takayasu's arteritis: a comparative analysis with diabetes mellitus. *Clin Exp Rheumatol* 2024; 43(4): 636-46. https://doi.org/10.55563/clinexprheumatol/gyo8xt
2. ZHOU Z, FANG C, WANG L *et al*.: Baricitinib for refractory Takayasu arteritis: a prospective cohort study in a tertiary referral centre. *RMD Open* 2024; 10(1): e003985. https://doi.org/10.1136/rmdopen-2023-003985
3. PARK SH, CHUNG JW, LEE JW, HAN MH, PARK JH: Carotid artery involvement in Takayasu's arteritis: evaluation of the activity by ultrasonography. *J Ultrasound Med* 2001; 20(4): 371-78. https://doi.org/10.7863/jum.2001.20.4.371
4. MARVISI C, BOLEK EC, AHLMAN MA *et al*.: Development of the Takayasu Arteritis Integrated Disease Activity Index. *Arthritis Care Res* (Hoboken) 2024; 76(4): 531-40. https://doi.org/10.1002/acr.25275
5. JIANG Z, LEFEBVRE F, ROSS C *et al*.: Variations in Takayasu arteritis characteristics in a cohort of patients with different racial backgrounds. *Semin Arthritis Rheum* 2022; 53: 151971. https://doi.org/10.1016/j.semarthrit.2022.151971
6. AESCHLIMANN FA, RAIMONDI F, LEINER T, AQUARO GD, SAADOUN D, GROTENHUIS HB: Overview of imaging in adult- and Childhood-onset Takayasu arteritis. *J Rheucatol* 2022; 49(4): 346-57. https://doi.org/10.3899/jrheum.210368
7. DEJACO C, RAMIRO S, BOND M *et al*.: EULAR recommendations for the use of imaging in large vessel vasculitis in clinical practice: 2023 update. *Ann Rheum Dis* 2024; 83(6): 741-51. https://doi.org/10.1136/ard-2023-224543
8. DELVINO P, BALDINI C, BONACINI M *et al*.: Systemic vasculitis: one year in review 2025. *Clin Exp Rheumatol* 2025; 43(4): 553-62. https://doi.org/10.55563/clinexprheumatol/oyqz1p
9. LOPEZ D, GUEVARA M: Use of ultrasound in the diagnosis and management of the vascu-

litides. *Curr Rheumatol Rep* 2020; 22(7): 31. https://doi.org/10.1007/s11926-020-00902-x
10. MA L, SUN Y, LIU Y *et al*.: A novel ultrasound-based score for assessing carotid artery activity in Takayasu's arteritis. *Clin Exp Rheumatol* 2025; 43(4): 647-54. https://doi.org/10.55563/clinexprheumatol/purgx3
11. DING J, WU D, HAN Q, ZHANG K, ZHENG Z, ZHU P: Follow-up contrast-enhanced ultrasonography of the carotid artery in patients with Takayasu arteritis: a retrospective study. *J Rheumatol* 2022; 49(11): 1242-49. https://doi.org/10.3899/jrheum.220114
12. SCHÄFER VS, JIN L, SCHMIDT WA: Imaging for diagnosis, monitoring, and outcome prediction of large vessel vasculitides. *Curr Rheumatol Rep* 2020; 22(11): 76. https://doi.org/10.1007/s11926-020-00955-y
13. SCHOEN S, ZHAO Z, ALVA A, HUANG C, CHEN S, ARVANITIS C: Morphological reconstruction improves microvessel mapping in super-resolution ultrasound. *IEEE Trans Ultrason Ferroelectr Freq Control* 2021; 68(6): 2141-49. https://doi.org/10.1109/tuffc.2021.3057540
14. HUANG B, YAN J, MORRIS M, SINNETT V, SOMAIAH N, TANG M-X: Acceleration-based kalman tracking for super-resolution ultrasound imaging in vivo. *IEEE Trans Ultrason Ferroelectr Freq Control* 2023; 70(12): 1739-48. https://doi.org/10.1109/tuffc.2023.3326863
15. HUANG X, YE H, HU Y *et al*.: Ultrasound super-resolution imaging for non-invasive assessment of microvessel in prostate lesion. *Cancer Imaging* 2025; 25(1): 1. https://doi.org/10.1186/s40644-024-00819-z
16. DEMENÉ C, ROBIN J, DIZEUX A *et al*.: Transcranial ultrafast ultrasound localization microscopy of brain vasculature in patients. *Nat Biomed Eng* 2021; 5(3): 219-28. https://doi.org/10.1038/s41551-021-00697-x
17. LEROY H, WANG LZ, JIMENEZ A *et al*.: Assessment of microvascular flow in human atherosclerotic carotid plaques using ultrasound localization microscopy. *EBioMedicine* 2025; 111: 105528. https://doi.org/10.1016/j.ebiom.2024.105528
18. BODARD S, DENIS L, HINGOT V *et al*.: Ultrasound localization microscopy of the human kidney allograft on a clinical ultrasound scanner. *Kidney Int* 2023; 103(5): 930-35. https://doi.org/10.1016/j.kint.2023.01.027
19. GOUDOT G, JIMENEZ A, MOHAMEDI N *et al*.: Vasa vasorum interna in the carotid wall of active forms of Takayasu arteritis evidenced by ultrasound localization microscopy. *Vasc Med* 2024; 29(3): 296-301. https://doi.org/10.1177/1358863x241228262
20. GOUDOT G, JIMENEZ A, MOHAMEDI N *et al*.: Assessment of Takayasu's arteritis activity by ultrasound localization microscopy. *EBioMedicine* 2023; 90: 104502. https://doi.org/10.1016/j.ebiom.2023.104502
21. AREND WP, MICHEL BA, BLOCH DA *et al*.: The American College of Rheumatology 1990 criteria for the classification of Takayasu arteritis. *Arthritis Rheum* 1990; 33(8): 1129-34. https://doi.org/10.1002/art.1780330811
22. RAFAILIDIS V, CHARITANTI A, TEGOS T, DESTANIS E, CHRYSSOGONIDIS I: Contrast-enhanced ultrasound of the carotid system: a review of the current literature. *J Ultrasound* 2017; 20(2): 97-109. https://doi.org/10.1007/s40477-017-0239-4
23. LI Z, ZHENG Z, DING J *et al*.: Contrast-enhanced ultrasonography for monitoring arterial inflammation in Takayasu arteritis. *J Rheumatol* 2019; 46(6): 616-22. https://doi.org/10.3899/jrheum.180701
24. KERR GS, HALLAHAN CW, GIORDANO J *et al*.: Takayasu arteritis. *Ann Intern Med* 1994; 120(11): 919-29. https://doi.org/10.7326/0003-4819-120-11-199406010-00004
25. KONG X, SUN Y, DAI X *et al*.: Treatment efficacy and safety of tofacitinib versus methotrexate in Takayasu arteritis: a prospective observational study. *Ann Rheum Dis* 2022; 81(1): 117-23. https://doi.org/10.1136/annrheumdis-2021-220832
26. DONG Y, WANG Y, WANG Y *et al*.: Ultrasonography and contrast-enhanced ultrasound for activity assessment in 115 patients with carotid involvement of Takayasu arteritis. *Mod Rheumatol* 2023; 33(5): 1007-15. https://doi.org/10.1093/mr/roac107
27. GIORDANA P, BAQUÉ-JUSTON MC, JEANDEL PY *et al*.: Contrast-enhanced ultrasound of carotid artery wall in Takayasu disease: first evidence of application in diagnosis and monitoring of response to treatment. *Circulation* 2011; 124(2): 245-47. https://doi.org/10.1161/circulationaha.110.006668
28. SCHINKEL AFL, VAN DEN OORD SCH, VAN DER STEEN AFW, VAN LAAR JAM, SIJBRANDS EJG: Utility of contrast-enhanced ultrasound for the assessment of the carotid artery wall in patients with Takayasu or giant cell arteritis. *Eur Heart J Cardiovasc Imaging* 2014; 15(5): 541-46. https://doi.org/10.1093/ehjci/jet243
29. HUANG Y, MA X, LI M, DONG H, WAN Y, ZHU J: Carotid contrast-enhanced ultrasonographic assessment of disease activity in Takayasu arteritis. *Eur Heart J Cardiovasc Imaging* 2019; 20(7): 789-95. https://doi.org/10.1093/ehjci/jey197
30. DENCKS S, SCHMITZ G: Ultrasound localization microscopy. *Z Med Phys* 2023; 33(3): 292-308. https://doi.org/10.1016/j.zemedi.2023.02.004
31. MA L-Y, LI C-L, MA L-L *et al*.: Value of contrast-enhanced ultrasonography of the carotid artery for evaluating disease activity in Takayasu arteritis. *Arthritis Res Ther* 2019; 21(1): 24. https://doi.org/10.1186/s13075-019-1813-2